Curr Cardiol Rep (2013) 15:337
DOI 10.1007/s11886-012-0337-z

CARDIAC PET, CT, AND MRI (S ACHENBACH, SECTION EDITOR)

PET and SPECT in Heart Failure

Christoph Rischpler · Stephan Nekolla · Markus Schwaiger

Published online: 22 January 2013

Abstract Heart failure is a serious condition with poor prognosis, which imposes an ever increasing burden on healthcare systems due to its rising prevalence. Nonetheless, physiological processes underlying heart failure remain poorly understood. In recent years, functional imaging such as gated CT has become available for routine clinical cardiology investigations. However, a maturation of nuclear imaging techniques such as PET and SPECT is now yielding new insights into the pathophysiological changes underlying heart failure, based on non-invasive measurements of myocardial blood flow, myocardial viability, sympathetic innervation, neoangiogenesis and matrix metalloproteinases activity. Investigations of these biomarkers have the potential to reveal early aspects of left ventricle remodeling; diagnosis at an earlier stage of heart failure promises to facilitate improved intervention and therapy guidance. Furthermore, nuclear imaging techniques are being developed to monitor and predict outcome of novel cell-based approaches for restorative therapy of heart failure.

Keywords Heart failure · Molecular imaging · PET · SPECT

This article is part of the Topical Collection on *Cardiac PET, CT, and MRI*

C. Rischpler · S. Nekolla · M. Schwaiger
Department of Nuclear Medicine, Technical University, Munich, Germany

C. Rischpler
e-mail: c.rischpler@tum.de

S. Nekolla
e-mail: stephan.nekolla@tum.de

C. Rischpler · S. Nekolla · M. Schwaiger (✉)
Klinikum rechts der Isar, Nuklearmedizinische Klinik und Poliklinik, Ismaninger Straße 22, 81675 München, Germany
e-mail: markus.schwaiger@tum.de

Introduction

Heart failure (HF) is a serious condition with high mortality and morbidity. In 2008 about 5.7 million people in the USA were suffering from HF [1] and worldwide about 23 million people are living with HF [2]. Approximately 1 % of people older than 65 years are affected by this disease, and the lifetime risk of people aged 40 years for subsequently developing HF is about 20 % [1, 3]. There has in recent years been a documented increase in the prevalence of HF of about 1‰ in men [4], whereas the rate of hospitalization due to HF has risen fourfold within a similar time period [3]. Although survival after HF diagnosis has improved considerably in recent years, the mortality rate within five years of diagnosis is still as high as 50 % [5, 6].

HF is a multifactorial complex disease that can be caused and perpetuated by several pre-existing disorders and risk factors. While hypertension, valve disease and coronary artery disease - especially myocardial infarction - were the most common causes until the 1970s, coronary artery disease and diabetes have subsequently become more important factors leading to the development of HF [7–10].

The etiology of HF is diverse and complex, but arises in general as a consequence of structural or functional cardiac diseases that compromise the left ventricular (LV) function. In response to this compromised function, different compensatory regulatory mechanisms are activated, which can in some measure compensate for the reduced pump function. However, in a chronic state of LV dysfunction, these compensatory mechanisms may come to exacerbate the underlying disease, ultimately leading to cardiac remodeling through hypertrophy and fibrosis of the myocardium [11].

For the purposes of diagnostics, exact staging, guidance of therapy, and determination of prognosis, it is necessary to acquire for each patient an integrated range of clinical information. Diverse non-invasive techniques are now available

for this evaluation. However, only nuclear medicine imaging has the potential to probe directly molecular processes of the myocardium and provide information about myocardial perfusion and metabolism, or to assess the sympathetic innervation of the heart; changes in these parameters accompany the progression of HF and LV dysfunction and are centrally implicated in the development, progression and maintenance of HF.

This review presents an overview on the current capabilities of nuclear medicine techniques for the metabolic characterization of the myocardium of patients at risk, or with overt HF. We present a comprehensive overview of PET and SPECT methods to evaluate myocardial blood flow and metabolism, and sympathetic innervation. In addition, we introduce and discuss novel concepts and tracers that promise to provide deeper insight into cellular and molecular mechanisms of HF than has been hitherto possible.

Nuclear Medicine Imaging in Heart Failure

Due to the success of PET in the oncological field, there is a wide availability of advanced PET instrumentation. Furthermore, today's PET instruments for nuclear medicine imaging, and increasingly also SPECT scanners, are usually equipped with a high resolution CT component. Morphological imaging by CT allows not only the exact anatomic localization of the PET or SPECT signal, but is also of critical importance for attenuation correction of quantitative nuclear medicine studies. The advent of hybrid PET/CT and SPECT/CT scanners have facilitated progress in molecular cardiology imaging.

Despite these technical innovations, myocardial perfusion imaging (MPI) remains the most conducted nuclear medicine application in the workup of patients with CAD or HF [12]. However, alternative imaging modalities are attaining greater importance; notably sympathetic imaging of the failing heart is increasingly used to obtain important information relevant to risk stratification, and prediction of ventricular arrhythmias or sudden cardiac death. Moreover, imaging of molecular processes in cardiac tissue is a "hot topic" in contemporary research, holding great promise for therapy guidance and evaluation of therapy response.

Nuclear Medicine Imaging of the Failing Heart Using Radionuclide Perfusion Tracers

Patients presenting with HF are initially classified based on the etiology of their disease, i.e., ischemic or non-ischemic cardiomyopathy. The diagnosis of HF is clear if prior myocardial infarction is reliably documented. However, non-ischemic cardiomyopathies can arise from a wide range of causes. Therefore, non-invasive differentiation of cardiomyopathies is critical for optimal treatment and accurate prognosis. Furthermore, patients with suspected ischemic HF may have to undergo catheterization, which is associated with a higher risk of death in patients with depressed LVEF [13]. No single imaging modality is suited to provide all the necessary information, but contemporary medical imaging offers a diverse toolbox for patient workup.

^{201}Thallium (^{201}Tl) perfusion imaging was found in one study to be relatively specific for the diagnosis of ischemic cardiomyopathy when a defect comprising 40 % or more of the LV circumference was detected [14]. In contrast, patients with non-ischemic cardiomyopathy typically showed defects of less than 20 % of image circumference. Another possible way to differentiate ischemic from non-ischemic cardiomyopathy is through assessment of myocardial wall motion by SPECT or PET. However, an exact differentiation is difficult by this approach, as both disease entities may manifest in hypokinesis [15, 16]. Danias et al. reported that gated ^{99m}Tc-sestamibi SPECT under exercise stress allows more accurate differentiation by assessment of perfusion defect scores and regional or segmental wall motion variability [17]. However, in other studies only the presence of severe and extensive perfusion defects under stress allowed the accurate differentiation between both disease entities; presence of mild stress perfusion defects may be ambiguous, as they can also occur in non-ischemic cardiomyopathy [18, 19]. Another potential marker of ischemic cardiomyopathy is the presence of myocardial ischemia [18, 20]. Her et al. demonstrated the diagnostic usefulness of ^{99m}Tc-sestamibi gated SPECT with adenosine challenge in patients with HF [20].

PET molecular imaging has also been investigated for the classification of HF patients. In a ^{11}C-palmitate PET study for the estimation of regional myocardial fatty acid myocardial utilization, Eisenberg et al. showed impressive visual differences between ischemic and non-ischemic cause of HF, and obtained differentiation with 80 % sensitivity and 100 % specificity [15]. Also, the combination of $^{13}NH_3$ PET for perfusion and ^{18}F-FDG PET for glucose metabolism has proven valuable for the classification of cardiomyopathy, with 100 % sensitivity and 80 % specificity [21].

SPECT Imaging Using ^{201}Tl or ^{99m}Tc-labeled Compounds

Several radionuclide imaging techniques are available for the evaluation of myocardial perfusion and cell membrane integrity. SPECT perfusion imaging still represents the majority of such scans in nuclear cardiology, due to the wide availability of SPECT cameras and perfusion tracers, simple acquisition protocols and their high cost-effectiveness [22].

Using SPECT MPI, myocardial perfusion defects can be located and assigned to particular vessels, with quantitation of their extent and severity [23]. Moreover, perfusion tracers are also widely used to identify zones of viable myocardium. The most often used radionuclide tracers for this purpose are ^{201}Tl, ^{99m}Tc-sestamibi and ^{99m}Tc-tetrofosmin, which are reviewed below.

^{201}Tl

The initial cellular uptake of ^{201}Tl is mediated by the Na^+/K^+ ATPase, but tracer deposition is dependent upon, and directly proportional to, the regional blood flow. The late phase of uptake reveals the integrity of the sarcolemmal membrane, which is an indicator of myocardial viability.

SPECT with ^{201}Tl MPI suffers from a disadvantage arising from its relatively long half-life of 73.1 hours, which imparts high radiation exposure to the patient in the range of 22.0 – 31.4 mSv (effective dose) depending on the protocol [24]. Since the long half-life limits the dose which can be administered to the patient, ^{201}Tl MPI gives lower image quality in comparison to that from other perfusion tracers [25].

Several studies have provided evidence that ^{201}Tl imaging is very well-suited for the detection of myocardial viability. In a recently published meta-analysis, the mean sensitivity and specificity of ^{201}Tl SPECT for the prediction of regional function improvement of LV function after revascularization were 86 % and 59 %, respectively [26]. The rather unsatisfactory specificity may arise because segments were classified as viable based on the threshold of >50 % tracer uptake although tracer uptake might be compromised by subendocardial scar tissue, which is not amenable to improve after revascularization therapy. Furthermore, it is notable that functional recovery after revascularization correlates well with the amount of ^{201}Tl uptake on late images, which is more specifically indicative of viability [27].

Revascularization in patients with poor LV function and significant amounts of viable myocardium has a Class IIa recommendation according to the ACC/AHA Guidelines [28]. However, the amount of viable myocardium necessary as a precondition for improved outcome after revascularization remains to be defined and further investigation is necessary.

^{99m}Tc-labeled Compounds

The most commonly used ^{99m}Tc-labeled perfusion tracers for nuclear cardiology are ^{99m}Tc-sestamibi and ^{99m}Tc-tetrofosmin. The shorter half-life of ^{99m}Tc (≈6 hours) compared to that of ^{201}Tl leads to more favorable dosimetry, with administration of higher doses yielding improved image quality, and permitting the acquisition of gated images. Furthermore, ^{99m}Tc is readily available from a generator, and decays with photon energy of about 140 keV, which results in less scatter and also less attenuation by soft tissue.

The lipophilic carrier molecules sestamibi and tetrofosmin diffuse rapidly across plasma membranes, and are retained within mitochondria of living cells due to the large negative membrane potential of intact, functional mitochondria. These properties suggest that ^{99m}Tc-sestamibi and ^{99m}Tc-tetrofosmin can be used for the determination of both myocardial perfusion and cellular viability. In many investigations, the radiotracer uptake is first quantified, and a threshold of 50-60 % of the maximal radiotracer uptake in dysfunctional segments is applied as viability criterion [26, 29]. Resting images are frequently obtained after nitrate administration so as to enhance myocardial blood flow and thus maximize tracer delivery downstream to severe stenosis [30]. Furthermore, ECG-gating of SPECT acquisitions can give improved detection of myocardial perfusion, LV function, and viability.

In a meta-analysis encompassing 20 studies using ^{99m}Tc-labeled tracers regional LV function improvement after revascularization was predicted with a sensitivity of 81 %, and specificity of 66 % [26]. However, a subanalysis of exclusively the nitrate-enhanced studies showed sensitivity of 86 % and specificity of 83 %, indicating improved accuracy in the condition of increased blood flow. Sciagrà et al. further evaluated the long-term prognostic value of nitrate-enhanced ^{99m}Tc-sestamibi imaging in patients with HF due to chronic CAD, who either underwent medical treatment, incomplete revascularization or complete revascularization [30]. Patients who obtained complete revascularization showed significantly better survival than did the other groups. Interestingly, the strongest predictor for subsequent cardiac events was the presence of non-revascularized, but viable and asynergic segments, which emerged as an ominous precondition for poor prognosis in HF patients.

PET Imaging Using N-13 Ammonia ($^{13}NH_3$) or Rubidium-82 (^{82}Rb)

PET MPI is emerging as a more frequently utilized method for the highly accurate detection of CAD. Benefiting from its greater spatial resolution and sensitivity, PET MPI may be superior to SPECT MPI with respect to image quality, interpretative confidence and inter-reader agreement [31, 32]. While SPECT images are usually assessed visually, or with semi-quantitative analysis, PET allows the absolute quantification of myocardial blood flow at rest or during pharmacological stress. Furthermore, the determination of flow reserve can be helpful in the differentiation between different underlying disease entities leading to HF.

Reduced perfusion of the myocardium, be it due to relevant stenoses in the coronaries or due to microvascular

dysfunction, may ultimately disrupt cellular integrity, leading to apoptosis and fibrotic replacement of the tissue. Less pronounced perfusion deficiency may perturb the metabolism of glucose and fatty acids in compromised tissue, which may in turn induce an abnormal contraction pattern of the heart [33].

Available PET radiotracers for clinical MPI include O-15 water, ^{82}Rb and $^{13}NH_3$ [34, 35]. Because of the short half-life of these radionuclides, serial measurements at rest and under stress conditions are feasible in a single setting. A relatively high first-pass extraction fraction even at high flow rates is a crucial property of PET MPI tracers, as low extraction would decrease accuracy of ischemia detection, and result in underestimation of blood flow [36]. O-15 water uniquely is freely diffusible between blood and tissue, i.e., has 100 % extraction. $^{13}NH_3$ and ^{82}Rb have lower extraction, which could result in underestimation of myocardial perfusion at higher flow rates. However, results of several studies with these radiotracers showed that myocardial blood flow is accurately quantified over a wide range of flow values [37–39]. Furthermore, the novel PET perfusion tracer ^{18}F-flurpiridaz seems to have favorable properties for clinical use [40]. The longer half-life of ^{18}F would enable many scans from a single bombardment and radiosynthesis.

When PET data are acquired in list mode, the subsequent reconstruction allows generation of conventional images for visual and semi-quantitative analysis. With ECG gating during acquisition, additional evaluation of LV functional parameters is possible. Furthermore, by employing a kinetic model as appropriate for the tracer, myocardial blood flow at rest and under stress can be highly reproducible quantified [41, 42].

PET MPI is proving invaluable for the characterization of flow defects in patients with HF arising from diverse causes. As expected, patients suffering from advanced CAD show a reduced myocardial flow reserve due to obstructive stenoses in the coronaries. In patients with ischemic heart disease, a reduced myocardial flow reserve was shown to have prognostic implications, being a more sensitive predictor for cardiac death than was reduced LVEF [43]. Interestingly, flow reserve in patients with CAD was found to be also reduced in areas supplied by non-stenotic vessels [44], suggesting a microvascular component. It was previously held that reduced myocardial blood flow in the failing heart is caused by reduced contractility and by mechanical factors such as high wall stress [45, 46]. However, results of several recent studies support the notion that microvascular dysfunction in HF is an independent predictor for the course of the disease and adverse outcome [47, 48]. A reduced myocardial blood flow has been detected in dilated cardiomyopathy, in the absence of overt HF [49]. Furthermore, patients with idiopathic dilated cardiomyopathy have a reduced coronary flow response to sympathetic stimulation as evoked by the cold pressure test when compared to a healthy control group [50]. Also, patients with idiopathic dilated cardiomyopathy and an impaired myocardial blood flow under hyperemic conditions have a poor prognosis [48]. Camici et al. reported that subjects suffering from hypertrophic cardiomyopathy had reduced myocardial flow reserve not only in hypertrophied septum but, interestingly, also in non-hypertrophied free walls [51], suggesting a global microvascular defect extending to seemingly healthy domains of the myocardium. A reduced global stress flow and myocardial flow reserve were independent factors for the prediction of cardiac death, worsening HF or sustained ventricular arrhythmias in patients with hypertrophic cardiomyopathy [47].

PET Viability Imaging Using ^{18}F-FDG

^{18}F-FDG PET viability imaging is regarded as the gold standard for myocardial viability assessment. It is based upon the principle that the radiolabeled glucose analog is trapped in tissue as a functional of the local rate of glucose metabolism. The tracer in circulation enters cardiomyocytes via the glucose transporters GLUT-1 and GLUT-4, and is then metabolized by the hexokinase to ^{18}F-FDG-6-phosphate, but proceeds no further in the glycolytic pathway, and is retained in cardiomyocytes due to its negative charge. In general, only viable tissue shows relevant glucose metabolism, such that ^{18}F-FDG PET can be used for viability assessment [52].

The uptake and metabolism of ^{18}F-FDG by the heart is substantially dependent on metabolic circumstances. In the fasting state, metabolism switches almost entirely to the oxidation of free fatty acids. However, PET studies suggest that there is a large heterogeneity of the myocardial ^{18}F-FDG uptake pattern in the fasting state [53]. In order to achieve reproducibly high signal intensities, several approaches are used to maximize glycolysis. In the most commonly used technique, glucose loading prior to ^{18}F-FDG injection stimulates insulin secretion, which enhances ^{18}F-FDG uptake in viable myocardium. Another approach is the simultaneous infusion of insulin and glucose, a technique known as hyperinsulinemic euglycemic clamping [54]. The latter approach has the advantage of overcoming reduced ^{18}F-FDG uptake, and thus, reduced image quality, in patients with impaired glucose tolerance or overt diabetes.

The assessment of both myocardial perfusion and viability is generally accepted to serve for distinguishing between viable and avital cardiac regions. Myocardial blood flow can be assessed using the PET perfusion tracers presented above and ^{18}F-FDG PET which provides a more specific index of viability than is afforded by the late phase of indirect “mitochondrial” tracers. Tissue with concomitantly

reduced blood flow and ^{18}F-FDG uptake, a state called perfusion/metabolism match, is considered to be avital, while reduced blood flow and preserved or even upregulated FDG uptake, a state known as perfusion/metabolism mismatch, is interpreted to reveal ischemic but viable tissue [55–57]. Upregulation of ^{18}F-FDG uptake in ischemically compromised myocardium is known to be associated with poor outcome [58]. Furthermore, the spatial extent of the mismatch area has therapeutic significance; revascularization in patients with a mismatch size of at least 5 % had superior outcome in a study by Di Carli et al. [59], while others report that a mismatch area of at least 7 % justified revascularization [60••]. An illustration of mismatch in a patient with hypoperfused but viable myocardium by ^{13}N-NH$_3$/^{18}F-FDG PET with the Siemens Biograph mMR at our institution for viability assessement is depicted in Fig. 1.

Initial PET viability studies proved that the extent of reversibility of wall motion abnormalities after CABG could be accurately predicted by PET ^{18}F-FDG imaging [61]. A recently published pooled analysis argued that ^{18}F-FDG is more sensitive (92 %) with respect to the prediction of recovery of regional function after revascularization than are other viability imaging techniques, such as dobutamine echocardiography (80 %), ^{201}Tl (87 %) and technetium-99 m scintigraphy (83 %) or MRI (84 %) [62]. Furthermore, angina and HF symptoms in those patients with a perfusion/metabolism mismatch to ^{13}N-NH$_3$/^{18}F-FDG PET improved significantly after revascularization [63], and the amount of viable myocardium as assessed by PET imaging, but not by dobutamine echocardiography, prior to coronary bypass grafting is predictive for the improvement of exercise capacity [64]. While case-controlled, prospective randomized studies are still lacking, a meta-analysis of cardiac imaging procedures for myocardial viability testing has suggested prognostic implications in chronic CAD patients with impaired LV function and myocardial viability [65]. Several studies found improved survival after revascularization in patients with documented mismatched viable cardiac regions [63, 66, 67]. In a study of pre-operative risk assessment, Haas et al. showed that patients who were selected for CABG on the basis of PET viability imaging in addition to coronary angiography had lower early mortality than did patients selected on the basis of coronary angiography alone (survival rate after 12 months: 97±3 % vs. 79±8 %, ($p<0.01$)) [67].

Thus, ^{18}F-FDG PET is of proven utility in predicting benefits from revascularization therapy. However, the required amount of viable myocardium which is critical to justify revascularization therapy is not well established.

Sympathetic Innervation

Activation of compensatory mechanisms mediated by the sympathetic nervous system may initially ameliorate the impaired LV function in patients with HF, but may at a later disease stage actually promote progression of cardiac remodeling and exacerbation of HF [11]. Furthermore, it is well-known that alterations in sympathetic signaling extend beyond the infarct area caused by myocardial ischemia suggesting that sympathetic nerve fibers are more prone to ischemic injury than are cardiomyocytes [68]. Other studies suggest that denervated but perfused myocardium, as occurs after acute or chronic myocardial ischemia, might represent an arrhythmogenic source, and potential cause of sudden cardiac death [69, 70].

Excessive availability of norepinephrine as well as down-regulation, dysfunction or desensitization of both post-synaptic beta-adrenoreceptors and the presynaptic uptake-1 mechanism in the myocardium are observed in patients with HF [71, 72]. These processes are thought to play a pivotal role in the progression of HF. Consequently, imaging of the sympathetic innervation has emerged as an important topic in molecular imaging.

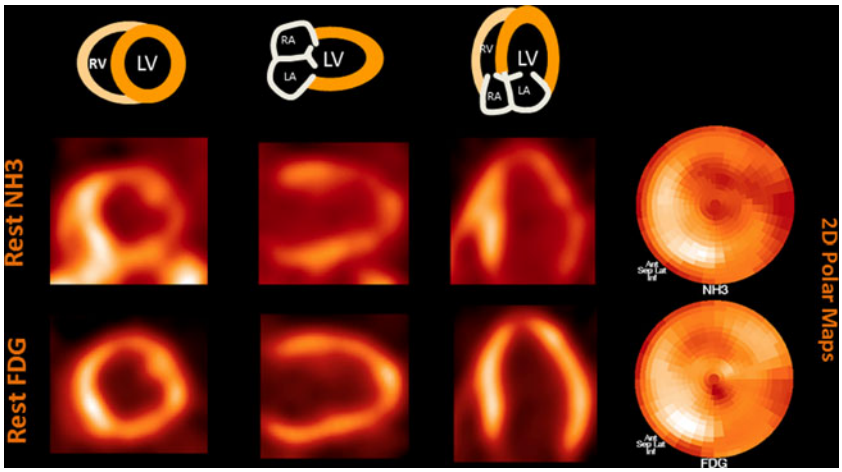

Fig. 1 Resting ^{13}NH$_3$ and ^{18}F-FDG PET short and long axes images of a patient who was referred for viability assessment to our institution. The scan was performed on the Siemens Biograph mMR, the first commercially available fully integrated PET/MR system. The anterolateral wall of the LV myocardium shows decreased ^{13}NH$_3$ retention while ^{18}F-FDG uptake is upregulated in the same area indicating hypoperfused but viable myocardium. The same phenomenon is also depicted in the 2D polar maps

SPECT

The most widely used radiotracer for SPECT imaging of cardiac sympathetic innervation is the noradrenaline analog ^{123}I-metaiodobenzylguanidine (MIBG) [73]. In humans, MIBG uptake is primarily mediated by the specific uptake-1, and only to a lesser degree by the less specific non-neural type-2 uptake site or by passive diffusion [74, 75]. Once inside the sympathetic nerve terminal, MIBG is retained within synaptic vesicles, but unlike noradrenaline, MIBG is not catabolized by monoamine oxidase (MAO) or catechol-O-methyltransferase (COMT), and has no biological effect on adrenergic receptors [76]. Usually, planar and SPECT imaging with MIBG is performed early (15–30 minutes) and late (3–4 hours) after tracer injection [77]. Using this protocol, the heart-to-mediastinum ratio (HMR) is calculated, serving as a highly reproducible, semiquantitative index for cardiac MIBG uptake. In addition, the wash-out rate from the myocardium is calculated from the ratio of early and late images as a surrogate marker for noradrenaline release, which reflects the state of sympathetic activation of the heart [78]. Furthermore, MIBG uptake images can be compared directly with perfusion images in order to investigate perfusion/innervation mismatch, which, as noted above, might have clinical implications [69, 79].

A strongly impaired sympathetic innervation of the heart in patients with HF is an independent prognostic predictor for cardiac events [80•, 81, 82]. In the ADMIRE-HF study, a prospective multicenter international trial examining 961 subjects, those patients with an MIBG HMR≥1.60 had 2-year probability for cardiac death of only 1.8 %, while those with HMR<1.6 had a 11.2 % risk [80•]. Subsequently, Travin et al. performed a multivariate analysis finding that HMR remained an independent predictor of cardiac and overall mortality [83]. In another study, HMR scores differed significantly between patients subsequently sustaining major cardiac events such as cardiac death, cardiac transplantation or potentially fatal arrhythmia, as compared to scores in patients with no major cardiac events (1.51 vs. 1.97; $p<0.0001$) [81]. Furthermore, ROC analysis showed a sensitivity of 84 % and a specificity of 60 % for predicting events with the optimal HMR threshold of 1.75. The MIBG washout rate also has proven prognostic implications; Kioka and colleagues showed that patients with a washout rate of 27 % or more were significantly more susceptible to sudden cardiac death [84]. In another study, a prospective comparison of MIBG findings with other factors found tracer washout rate to be an independent predictor of sudden cardiac death, irrespective of left ventricular ejection fraction [85]. It thus seems likely that MIBG SPECT may be a valuable tool to identify those HF patients who might need an implantable cardioverter defibrillator (ICD), given that previous studies showed the current criteria of LVEF≤35 % to be a suboptimal differentiator; most such patients would never experience an event triggering their ICD [86, 87].

In several studies MIBG cardiac imaging has been used for monitoring therapy with drugs that are typically prescribed to HF patients [88]. While routine therapy monitoring of well-known medications may be unlikely, given the relatively high SPECT imaging costs, MIBG imaging might be valuable for the validation of therapeutic response with investigational drugs. Drawing from the experience with oncology, MIBG imaging might be useful in following treatment with specific agents expected to bring benefits only in specific cases. These considerations notwithstanding, MIBG imaging is a worthy, widely available and well-established research tool.

PET

Several PET radiotracers for the assessment of the myocardial sympathetic innervation are available, among which ^{11}C-hydroxyephedrine (HED) is the most commonly used. Like MIBG, HED is a NE analog entering sympathetic terminals via the noradrenaline transporter, with a small additional component via the non-specific type-2 transport mechanism [89, 90] and is not metabolized by MAO and COMT. ^{11}C-epinephrine (EPI) is thought to be superior to HED, since it traces the entire pathway of catecholamine uptake, metabolism and vesicular storage, but has hitherto mainly been employed in pre-clinical research [91, 92]. In a study by Münch et al. EPI was directly compared to HED in healthy volunteers and patients after heart transplantation [89]. Interestingly, retention of EPI exceeded that of HED in normal hearts, but retention of EPI was lower than that of HED in transplanted (denervated) hearts, presumably reflecting lower non-specific uptake. Consequently, EPI might have inherently higher sensitivity to detect changes in sympathetic innervation of the heart.

Another interesting tracer is ^{11}C-phenylephrine (PHEN), which is also a substrate for MAO and is thought to be valuable in the assessment of vesicular leakage [93]. In a validation study of PHEN relative to HED in healthy humans, the two tracers gave initial uptake images of similar quality and uniformity [94]. However PHEN showed much faster washout, as might be expected for an MAO substrate. This property of PHEN allows calculation of storage half-life, which is potentially useful additional information about the functional integrity of the cardiac sympathetic innervation [94].

Despite the useful properties of EPI and PHEN, most human PET studies have used HED. Not only is global myocardial HED retention reduced in patients with HF, but there is also a distinct regional pattern of this reduction, predominantly in apical and inferoapical regions [95, 96]. Furthermore, the extent of reduced HED uptake in the

failing heart parallels the individual patient's NYHA class and ejection fraction [95], and reduced HED uptake was an independent predictor for the combined end-point of death or cardiac transplantation [97]. In a study investigating the effect of exercise training on sympathetic innervation in patient with chronic HF, the exercise intervention increased global HED uptake, suggesting a normalization of the compensatory autonomic nervous imbalance in HF [98]. In another study, sympathetic innervation, as well as oxidative metabolism and contractile function of patients suffering from idiopathic dilated cardiomyopathy were studied and HED retention proved to be the closest independent determinant of LVEF [99].

An illustration of a patient who was revascularized due to myocardial infarction and who was subsequently imaged by NH3/HED PET is shown in Fig. 2.

Potential Applications and Advances in Nuclear Imaging of the Failing Heart

^{18}F-galacto-RGD (RGD) – a Novel Angiogenesis Tracer

The initiation of LV remodeling could potentially be targeted for preventative therapy. Consequently, biomarkers are being developed for aspects of the complex healing and remodeling process after myocardial infarction, e.g., inflammation, angiogenesis, fibroblast proliferation or collagen deposition [100]. Among the most compelling targets are the integrins, which represent important proteins with regards to cell migration, cell proliferation, cell survival and differentiation [101]. ^{18}F-fluoro-galacto-RGD (RGD) has been developed as a PET ligand with high affinity for $\alpha_v\beta_3$ integrin receptors [101]. Using this ligand, the expression of $\alpha_v\beta_3$ integrin has already been investigated in different animal models of myocardial infarction, and a very preliminary study has been made in humans [102–104]. In a rat model of permanent coronary occlusion, $\alpha_v\beta_3$ integrins binding was lowest in myocardium of rats with an increase of at least 20 % of the EDV as assessed by MRI indicating that $\alpha_v\beta_3$ integrin expression might prove valuable for monitoring myocardial repair after MI [105]. These promising preclinical findings set the stage for investigation of remodeling processes and the prediction of HF onset in patients.

Matrix Metalloproteinases (MMP)

It has been recognized that changes in the extracellular matrix accompany the process of LV remodeling in the failing heart. In particular, a group of extracellular degradative enzymes known as the matrix metalloproteinases (MMP) are thought to play a pivotal role in HF [106]. The induction of MPP transcription is increased by activation of protein kinase C [107, 108], a process which can be activated by catecholamines, angiotensin II and endothelin [106, 109]. In a mouse model of myocardial infarction imaging of the upregulation of MMPs was demonstrated using the MMP ligand ^{111}In-RP782 [110]. Interestingly, MMP labeling was increased not only in the infarct area but also, albeit to a lesser degree, in the remote myocardium. Animal studies suggest that an intervention reducing MMP activity should attenuate the process of LV remodeling [111]. Sahul et al. demonstrated the feasibility of a noninvasive hybrid SPECT/CT imaging approach for assessing MMP activation with the ligand ^{99m}Tc-RP805, all in conjunction with cine MR for the investigation of LV deformation. Interestingly, elevated ^{99m}Tc-RP805 uptake was observed in the whole heart early after MI induction, but not in a simple reciprocal manner relative to myocardial perfusion as assessed by ^{201}Tl. The authors concluded that their approach might be useful for the prediction LV remodeling after MI [112].

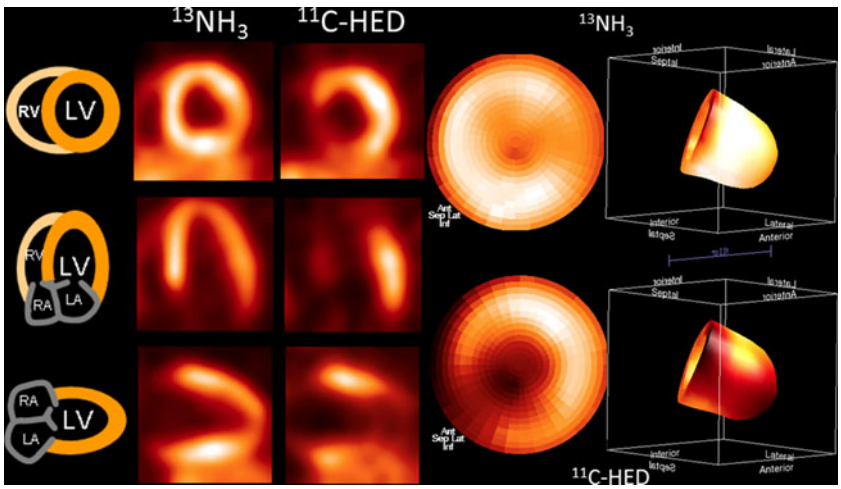

Fig. 2 Reduced HED retention despite normal NH3 uptake indicating denervated but perfused myocardium in a patient who was imaged after revascularization therapy due to myocardial infarction

Cell Tracking in Cell-Based Therapy Approaches

Recent Studies of apoptosis in failed human hearts found apoptosis rates of less than 1 % [113]. Impaired contractility and function of the affected myocardium increases in proportion to drop-out of cardiomyocytes. Cell transplantation presents a possible approach to overcome this loss. As the heart is in constant motion and also due to adverse conditions in the microenvironment at the grafting site, at least 30 % of the transplanted cells may be lost [114, 115]. Thus, cell labeling and noninvasive tracking are important techniques to gain a better understanding of the molecular mechanisms affecting cell biodistribution, homing, and engraftment.

PET and SPECT methods may prove valuable for cell-tracking, as they offer higher sensitivity as compared to MRI, and have the potential to also image functional aspects of cells, e.g., not just morphology but also viability. Two different approaches have mainly been used for cell labeling with radionuclides: (1) direct labeling of cells using radioactive tracers and (2) reporter gene imaging, whereby a gene transfected to cells expresses enzymes or receptors which are imaged with radiotracers. The latter procedure offers some advantages with respect to longitudinal imaging, in that detection is not limited by the half-life of the radiotracer. Furthermore, daughter cells of dividing cells should still express the reporter gene, and only viable cells express the reporter gene. Finally, loss of cell viability due to radiotoxicity [116] can be avoided. The reporter gene approach has already been applied successfully at our institution in both small and large animal models of heart disease [117, 118].

Despite its several advantages, the reporter gene approach is complex and time-consuming, and has not yet seen translation into human studies because of ethics considerations arising from the oncogenic potential of viral transfection vectors. Consequently, direct cell labeling is presently more accessible for clinical applications. Cells may be labeled directly using ^{111}In-oxyquinoline or ^{99m}Tc-hexamethylpropylene for SPECT imaging, or ^{18}F-FDG, which represent a commonly used PET approach for cell monitoring, although its applicability is limited by the two-hour half-life [119]. In the first human heart study applying the ^{18}F-FDG labeling technique, unselected bone marrow cells were infused in a coronary artery after revascularization in patients with NSTEMI [120]. About 1.3 – 2.6 % of the infused cells were acutely retained in the infarcted myocardium. This promising result illustrates the potential application of cell tracking in monitoring of patients treated after MI. However, it remains to be elucidated if the extent of acute cell retention has prognostic implications regarding LV remodeling and progression to HF.

Conclusion

The incidence of HF is steadily increasing in developed countries. Given the high morbidity and mortality, the prognosis of HF patients is worse than for common types of cancer. There is an urgent need for improved staging, improved guidance of therapy and determination of prognosis. Although a variety of imaging techniques are available for assessing HF, nuclear medical imaging techniques such as SPECT and PET uniquely offer the potential to assess molecular aspects of heart functional parameters. While ^{18}F-FDG PET represents the gold standard for viability assessment of compromised myocardium, $^{13}NH_3$ and ^{82}Rb perfusion PET as well as traditional SPECT perfusion tracers inform with relatively high sensitivity and specificity predictions about the regional LV function improvement to be obtained after revascularization. The assessment of sympathetic innervation by molecular techniques provides valuable information on outcome of patients, and can guide the decision to implant an ICD in patients with a high probability of sudden cardiac death. The development of radiotracers targeting non-traditional biomarkers of neoangiogenesis or MMPs is furnishing deeper insight into molecular processes of LV remodeling and HF. Last but not least, radionuclide techniques have been developed for monitoring intramyocardial cell transplantation as a restorative treatment for HF.

Acknowledgments The authors thank Dr. Paul Cumming for professional editing services.

Disclosure Conflicts of interest: C. Rischpler: none; S. Nekolla: none; M. Schwaiger: research grant from Siemens AG; Speakers bureau Siemens AG, General Electric Company.

References

Papers of particular interest, published recently, have been highlighted as:
- • Of importance
- •• Of major importance

1. Roger VL, Go AS, Lloyd-Jones DM, et al. Heart disease and stroke statistics–2011 update: a report from the American Heart Association. Circulation. 2011;123(4):e18–209.
2. McMurray JJ, Petrie MC, Murdoch DR, Davie AP. Clinical epidemiology of heart failure: public and private health burden. Eur Heart J. 1998;19(Suppl P):9–16.
3. Lloyd-Jones DM, Larson MG, Leip EP, et al. Lifetime risk for developing congestive heart failure: the Framingham Heart Study. Circulation. 2002;106(24):3068–72.
4. McCullough PA, Philbin EF, Spertus JA, Kaatz S, Sandberg KR, Weaver WD. Confirmation of a heart failure epidemic: findings from the Resource Utilization Among Congestive Heart Failure (REACH) study. J Am Coll Cardiol. 2002;39 (1):60–9.

5. Levy D, Kenchaiah S, Larson MG, et al. Long-term trends in the incidence of and survival with heart failure. N Engl J Med. 2002;347(18):1397–402.
6. Roger VL, Weston SA, Redfield MM, et al. Trends in heart failure incidence and survival in a community-based population. JAMA. 2004;292(3):344–50.
7. Ho KK, Pinsky JL, Kannel WB, Levy D. The epidemiology of heart failure: the Framingham Study. J Am Coll Cardiol. 1993;22 (4 Suppl A):6A–13.
8. Levy D, Larson MG, Vasan RS, Kannel WB, Ho KK. The progression from hypertension to congestive heart failure. JAMA. 1996;275(20):1557–62.
9. Kannel WB, Ho K, Thom T. Changing epidemiological features of cardiac failure. Br Heart J. 1994;72(2 Suppl):S3–9.
10. Gheorghiade M, Bonow RO. Chronic heart failure in the United States: a manifestation of coronary artery disease. Circulation. 1998;97(3):282–9.
11. McMurray JJ, Pfeffer MA. Heart failure. Lancet. 2005;365 (9474):1877–89.
12. Hendel RC, Berman DS, Di Carli MF, et al. ACCF/ASNC/ACR/AHA/ASE/SCCT/SCMR/SNM 2009 Appropriate Use Criteria for Cardiac Radionuclide Imaging: A Report of the American College of Cardiology Foundation Appropriate Use Criteria Task Force, the American Society of Nuclear Cardiology, the American College of Radiology, the American Heart Association, the American Society of Echocardiography, the Society of Cardiovascular Computed Tomography, the Society for Cardiovascular Magnetic Resonance, and the Society of Nuclear Medicine. J Am Coll Cardiol. 2009;53(23):2201–29.
13. Davis K, Kennedy JW, Kemp Jr HG, Judkins MP, Gosselin AJ, Killip T. Complications of coronary arteriography from the Collaborative Study of Coronary Artery Surgery (CASS). Circulation. 1979;59(6):1105–12.
14. Bulkley BH, Hutchins GM, Bailey I, Strauss HW, Pitt B. Thallium 201 imaging and gated cardiac blood pool scans in patients with ischemic and idiopathic congestive cardiomyopathy. A clinical and pathologic study. Circulation. 1977;55(5):753–60.
15. Eisenberg JD, Sobel BE, Geltman EM. Differentiation of ischemic from nonischemic cardiomyopathy with positron emission tomography. Am J Cardiol. 1987;59(15):1410–4.
16. Boucher CA, Fallon JT, Johnson RA, Yurchak PM. Cardiomyopathic syndrome caused by coronary artery disease. III: prospective clinicopathological study of its prevalence among patients with clinically unexplained chronic heart failure. Br Heart J. 1979;41(5):613–20.
17. Danias PG, Ahlberg AW, Clark 3rd BA, et al. Combined assessment of myocardial perfusion and left ventricular function with exercise technetium-99m sestamibi gated single-photon emission computed tomography can differentiate between ischemic and nonischemic dilated cardiomyopathy. Am J Cardiol. 1998;82(10):1253–8.
18. Yao SS, Qureshi E, Nichols K, Diamond GA, Depuey EG, Rozanski A. Prospective validation of a quantitative method for differentiating ischemic versus nonischemic cardiomyopathy by technetium-99m sestamibi myocardial perfusion single-photon emission computed tomography. Clin Cardiol. 2004;27 (11):615–20.
19. Wu YW, Yen RF, Chieng PU, Huang PJ. Tl-201 myocardial SPECT in differentiation of ischemic from nonischemic dilated cardiomyopathy in patients with left ventricular dysfunction. J Nucl Cardiol. 2003;10(4):369–74.
20. Her SH, Yoon HJ, Lee JM, et al. Adenosine Tc-99m tetrofosmin SPECT in differentiation of ischemic from nonischemic cardiomyopathy in patients with LV systolic dysfunction. Clin Nucl Med. 2008;33(7):459–63.
21. Mody FV, Brunken RC, Stevenson LW, Nienaber CA, Phelps ME, Schelbert HR. Differentiating cardiomyopathy of coronary artery disease from nonischemic dilated cardiomyopathy utilizing positron emission tomography. J Am Coll Cardiol. 1991;17 (2):373–83.
22. Marcassa C, Bax JJ, Bengel F, et al. Clinical value, cost-effectiveness, and safety of myocardial perfusion scintigraphy: a position statement. Eur Heart J. 2008;29(4):557–63.
23. Underwood SR, Anagnostopoulos C, Cerqueira M, et al. Myocardial perfusion scintigraphy: the evidence. Eur J Nucl Med Mol Imaging. 2004;31(2):261–91.
24. Gaemperli O, Bengel FM, Kaufmann PA. Cardiac hybrid imaging. Eur Hear J. 2011;32(17):2100–8.
25. Kapur A, Latus KA, Davies G, et al. A comparison of three radionuclide myocardial perfusion tracers in clinical practice: the ROBUST study. Eur J Nucl Med Mol Imaging. 2002;29 (12):1608–16.
26. Schinkel AF, Poldermans D, Elhendy A, Bax JJ. Assessment of myocardial viability in patients with heart failure. J Nucl Med. 2007;48(7):1135–46.
27. Perrone-Filardi P, Pace L, Prastaro M, et al. Assessment of myocardial viability in patients with chronic coronary artery disease. Rest-4-hour-24-hour 201Tl tomography versus dobutamine echocardiography. Circulation. 1996;94(11):2712–9.
28. Eagle KA, Guyton RA, Davidoff R, et al. ACC/AHA 2004 guideline update for coronary artery bypass graft surgery: summary article: a report of the American College of Cardiology/American Heart Association Task Force on Practice Guidelines (Committee to Update the 1999 Guidelines for Coronary Artery Bypass Graft Surgery). Circulation. 2004;110(9):1168–76.
29. Schneider CA, Voth E, Gawlich S, et al. Significance of rest technetium-99m sestamibi imaging for the prediction of improvement of left ventricular dysfunction after Q wave myocardial infarction: importance of infarct location adjusted thresholds. J Am Coll Cardiol. 1998;32(3):648–54.
30. Sciagra R, Pellegri M, Pupi A, et al. Prognostic implications of Tc-99m sestamibi viability imaging and subsequent therapeutic strategy in patients with chronic coronary artery disease and left ventricular dysfunction. J Am Coll Cardiol. 2000;36(3):739–45.
31. Bateman TM, Heller GV, McGhie AI, et al. Diagnostic accuracy of rest/stress ECG-gated Rb-82 myocardial perfusion PET: comparison with ECG-gated Tc-99m sestamibi SPECT. J Nucl Cardiol. 2006;13(1):24–33.
32. Flotats A, Bravo PE, Fukushima K, Chaudhry MA, Merrill J, Bengel FM. (82)Rb PET myocardial perfusion imaging is superior to (99m)Tc-labelled agent SPECT in patients with known or suspected coronary artery disease. Eur J Nucl Med Mol Imaging. 2012;39(8):1233–9.
33. Murphy ML, Kane JJ, Peng CF, Straub KD. Wall motion and metabolic changes after coronary occlusion and reperfusion. J Surg Res. 1982;32(2):143–9.
34. Higuchi T, Bengel FM. Cardiovascular nuclear imaging: from perfusion to molecular function: non-invasive imaging. Heart. 2008;94(6):809–16.
35. Heller GV, Calnon D, Dorbala S. Recent advances in cardiac PET and PET/CT myocardial perfusion imaging. J Nucl Cardiol. 2009;16(6):962–9.
36. Yoshida K, Mullani N, Gould KL. Coronary flow and flow reserve by PET simplified for clinical applications using rubidium-82 or nitrogen-13-ammonia. J Nucl Med. 1996;37 (10):1701–12.
37. Bergmann SR, Fox KA, Rand AL, et al. Quantification of regional myocardial blood flow in vivo with H215O. Circulation. 1984;70(4):724–33.
38. Bellina CR, Parodi O, Camici P, et al. Simultaneous in vitro and in vivo validation of nitrogen-13-ammonia for the assessment of regional myocardial blood flow. J Nucl Med. 1990;31(8):1335–43.

39. Lautamaki R, George RT, Kitagawa K, et al. Rubidium-82 PET-CT for quantitative assessment of myocardial blood flow: validation in a canine model of coronary artery stenosis. Eur J Nucl Med Mol Imaging. 2009;36(4):576–86.
40. Rischpler C, Park MJ, Fung GS, Javadi M, Tsui BM, Higuchi T. Advances in PET myocardial perfusion imaging: F-18 labeled tracers. Ann Nucl Med. 2012;26(1):1–6.
41. El Fakhri G, Kardan A, Sitek A, et al. Reproducibility and accuracy of quantitative myocardial blood flow assessment with (82)Rb PET: comparison with (13)N-ammonia PET. J Nucl Med. 2009;50(7):1062–71.
42. Nitzsche EU, Choi Y, Czernin J, Hoh CK, Huang SC, Schelbert HR. Noninvasive quantification of myocardial blood flow in humans. A direct comparison of the [13N]ammonia and the [15O]water techniques. Circulation. 1996;93(11):2000–6.
43. Tio RA, Dabeshlim A, Siebelink HM, et al. Comparison between the prognostic value of left ventricular function and myocardial perfusion reserve in patients with ischemic heart disease. J Nucl Med. 2009;50(2):214–9.
44. Legrand V, Mancini GB, Bates ER, Hodgson JM, Gross MD, Vogel RA. Comparative study of coronary flow reserve, coronary anatomy and results of radionuclide exercise tests in patients with coronary artery disease. J Am Coll Cardiol. 1986;8(5):1022–32.
45. Weiss MB, Ellis K, Sciacca RR, Johnson LL, Schmidt DH, Cannon PJ. Myocardial blood flow in congestive and hypertrophic cardiomyopathy: relationship to peak wall stress and mean velocity of circumferential fiber shortening. Circulation. 1976;54 (3):484–94.
46. Nitenberg A, Foult JM, Blanchet F, Zouioueche S. Multifactorial determinants of reduced coronary flow reserve after dipyridamole in dilated cardiomyopathy. Am J CardiolAm J Cardiol. 1985;55 (6):748–54.
47. Cecchi F, Olivotto I, Gistri R, Lorenzoni R, Chiriatti G, Camici PG. Coronary microvascular dysfunction and prognosis in hypertrophic cardiomyopathy. N Engl J Med. 2003;349(11):1027–35.
48. Neglia D, Michelassi C, Trivieri MG, et al. Prognostic role of myocardial blood flow impairment in idiopathic left ventricular dysfunction. Circulation. 2002;105(2):186–93.
49. Neglia D, Parodi O, Gallopin M, et al. Myocardial blood flow response to pacing tachycardia and to dipyridamole infusion in patients with dilated cardiomyopathy without overt heart failure. A quantitative assessment by positron emission tomography. Circulation. 1995;92(4):796–804.
50. Drzezga AE, Blasini R, Ziegler SI, Bengel FM, Picker W, Schwaiger M. Coronary microvascular reactivity to sympathetic stimulation in patients with idiopathic dilated cardiomyopathy. J Nucl Med. 2000;41(5):837–44.
51. Camici P, Chiriatti G, Lorenzoni R, et al. Coronary Vasodilation Is Impaired in Both Hypertrophied and Nonhypertrophied Myocardium of Patients with Hypertrophic Cardiomyopathy - a Study with N-13 Ammonia and Positron Emission Tomography. J Am Coll Cardiol. 1991;17(4):879–86.
52. Ghosh N, Rimoldi OE, Beanlands RS, Camici PG. Assessment of myocardial ischaemia and viability: role of positron emission tomography. Eur Heart J. 2010;31(24):2984–95.
53. Inglese E, Leva L, Matheoud R, et al. Spatial and temporal heterogeneity of regional myocardial uptake in patients without heart disease under fasting conditions on repeated whole-body 18F-FDG PET/CT. J Nucl Med. 2007;48(10):1662–9.
54. Fallavollita JA. Spatial heterogeneity in fasting and insulin-stimulated (18)F-2-deoxyglucose uptake in pigs with hibernating myocardium. Circulation. 2000;102(8):908–14.
55. Depre C, Vanoverschelde JL, Taegtmeyer H. Glucose for the heart. Circulation. 1999;99(4):578–88.
56. McNulty PH, Jagasia D, Cline GW, et al. Persistent changes in myocardial glucose metabolism in vivo during reperfusion of a limited-duration coronary occlusion. Circulation. 2000;101 (8):917–22.
57. Lopaschuk GD, Stanley WC. Glucose metabolism in the ischemic heart. Circulation. 1997;95(2):313–5.
58. Beanlands RSB, Hendry PJ, Masters RG, deKemp RA, Woodend K, Ruddy TD. Delay in revascularization is associated with increased mortality rate in patients with severe left ventricular dysfunction and viable myocardium on fluorine 18-fuorodeoxyglucose positron emission tomography imaging. Circulation. 1998;98(19):Ii51–6.
59. Di Carli MF, Davidson M, Little R, et al. Value of metabolic imaging with positron emission tomography for evaluating prognosis in patients with coronary artery disease and left ventricular dysfunction. Am J Cardiol. 1994;73(8):527–33.
60. •• D'Egidio G, Nichol G, Williams KA, et al. Increasing Benefit From Revascularization Is Associated With Increasing Amounts of Myocardial Hibernation A Substudy of the PARR-2 Trial. Jacc-Cardiovasc Imag. 2009;2(9):1060–8. *Important study demonstrating that patients suffering from ischemic cardiomyopathy with larger amounts of mismatch have a better outcome after revascularization*.
61. Tillisch J, Brunken R, Marshall R, et al. Reversibility of cardiac wall-motion abnormalities predicted by positron tomography. N Engl J Med. 1986;314(14):884–8.
62. Schinkel AF, Bax JJ, Poldermans D, Elhendy A, Ferrari R, Rahimtoola SH. Hibernating myocardium: diagnosis and patient outcomes. Curr Probl Cardiol. 2007;32(7):375–410.
63. Di Carli MF, Maddahi J, Rokhsar S, et al. Long-term survival of patients with coronary artery disease and left ventricular dysfunction: implications for the role of myocardial viability assessment in management decisions. J Thorac Cardiovasc Surg. 1998;116 (6):997–1004.
64. Marwick TH, Zuchowski C, Lauer MS, Secknus MA, Williams J, Lytle BW. Functional status and quality of life in patients with heart failure undergoing coronary bypass surgery after assessment of myocardial viability. J Am Coll Cardiol. 1999;33 (3):750–8.
65. Allman KC, Shaw LJ, Hachamovitch R, Udelson JE. Myocardial viability testing and impact of revascularization on prognosis in patients with coronary artery disease and left ventricular dysfunction: a meta-analysis. J Am Coll Cardiol. 2002;39(7):1151–8.
66. Dicarli MF, Asgarzadie F, Schelbert HR, et al. Quantitative Relation between Myocardial Viability and Improvement in Heart-Failure Symptoms after Revascularization in Patients with Ischemic Cardiomyopathy. Circulation. 1995;92(12):3436–44.
67. Haas F, Haehnel CJ, Picker W, et al. Preoperative positron emission tomographic viability assessment and perioperative and postoperative risk in patients with advanced ischemic heart disease. J Am Coll Cardiol. 1997;30(7):1693–700.
68. Matsunari I, Schricke U, Bengel FM, et al. Extent of cardiac sympathetic neuronal damage is determined by the area of ischemia in patients with acute coronary syndromes. Circulation. 2000;101(22):2579–85.
69. Sasano T, Abraham MR, Chang KC, et al. Abnormal sympathetic innervation of viable myocardium and the substrate of ventricular tachycardia after myocardial infarction. J Am Coll Cardiol. 2008;51(23):2266–75.
70. Bertini M, Schalij MJ, Bax JJ, Delgado V. Emerging role of multimodality imaging to evaluate patients at risk for sudden cardiac death. Circ Cardiovasc Imaging. 2012;5(4):525–35.
71. Bohm M, La Rosee K, Schwinger RH, Erdmann E. Evidence for reduction of norepinephrine uptake sites in the failing human heart. J Am Coll Cardiol. 1995;25(1):146–53.
72. Eisenhofer G, Friberg P, Rundqvist B, et al. Cardiac sympathetic nerve function in congestive heart failure. Circulation. 1996;93 (9):1667–76.

73. The MICAD Research Team. Meta-[radioiodinated]iodobenzylguanidine. Molecular Imaging and Contrast Agent Database (MICAD). Bethesda (MD): ational Center for Biotechnology Information (US). 2004–2012.
74. Dae MW, De Marco T, Botvinick EH, et al. Scintigraphic assessment of MIBG uptake in globally denervated human and canine hearts–implications for clinical studies. J Nucl Med. 1992;33 (8):1444–50.
75. Estorch M, Camprecios M, Flotats A, et al. Sympathetic reinnervation of cardiac allografts evaluated by 123I-MIBG imaging. J Nucl Med. 1999;40(6):911–6.
76. Wieland DM, Brown LE, Rogers WL, et al. Myocardial imaging with a radioiodinated norepinephrine storage analog. J Nucl Med. 1981;22(1):22–31.
77. Carrio I. Cardiac neurotransmission imaging. J Nucl Med. 2001;42(7):1062–76.
78. Flotats A, Carrio I. Cardiac neurotransmission SPECT imaging. J Nucl Cardiol. 2004;11(5):587–602.
79. Simoes MV, Barthel P, Matsunari I, et al. Presence of sympathetically denervated but viable myocardium and its electrophysiologic correlates after early revascularised, acute myocardial infarction. Eur Heart J. 2004;25(7):551–7.
80. • Jacobson AF, Senior R, Cerqueira MD, et al. Myocardial iodine-123 meta-iodobenzylguanidine imaging and cardiac events in heart failure. Results of the prospective ADMIRE-HF (AdreView Myocardial Imaging for Risk Evaluation in Heart Failure) study. J Am Coll Cardiol. 2010;55(20):2212–21. *First, large prospective study confirming the usefulness of cardiac sympathetic nerve imaging with 123I-MIBG as an independent prognostic predictor for cardiac events*.
81. Agostini D, Verberne HJ, Burchert W, et al. I-123-mIBG myocardial imaging for assessment of risk for a major cardiac event in heart failure patients: insights from a retrospective European multicenter study. Eur J Nucl Med Mol Imaging. 2008;35 (3):535–46.
82. Verberne HJ, Brewster LM, Somsen GA, van Eck-Smit BL. Prognostic value of myocardial 123I-metaiodobenzylguanidine (MIBG) parameters in patients with heart failure: a systematic review. Eur Heart J. 2008;29(9):1147–59.
83. Travin M, Ananthasubramaniam K, Henzlova MJ, Clements IP, Amanullah A, Jacobson AF. Imaging of Myocardial Sympathetic Innervation for Prediction of Cardiac and All-cause Mortality in Heart Failure Patients: analyses From the ADMIRE-HF Trial. Circulation. 2009;120(18):S350–S50.
84. Kioka H, Yamada T, Mine T, et al. Prediction of sudden death in patients with mild-to-moderate chronic heart failure by using cardiac iodine-123 metaiodobenzylguanidine imaging. Heart. 2007;93(10):1213–8.
85. Tamaki S, Yamada T, Okuyama Y, et al. Cardiac iodine-123 metaiodobenzylguanidine imaging predicts sudden cardiac death independently of left ventricular ejection fraction in patients with chronic heart failure and left ventricular systolic dysfunction: results from a comparative study with signal-averaged electrocardiogram, heart rate variability, and QT dispersion. J Am Coll Cardiol. 2009;53(5):426–35.
86. Buxton AE, Lee KL, Hafley GE, et al. Limitations of ejection fraction for prediction of sudden death risk in patients with coronary artery disease: lessons from the MUSTT study. J Am Coll Cardiol. 2007;50(12):1150–7.
87. Desai AS, Fang JC, Maisel WH, Baughman KL. Implantable defibrillators for the prevention of mortality in patients with nonischemic cardiomyopathy: a meta-analysis of randomized controlled trials. JAMA. 2004;292(23):2874–9.
88. Carrio I, Cowie MR, Yamazaki J, Udelson J, Camici PG. Cardiac sympathetic imaging with mIBG in heart failure. JACC Cardiovasc Imaging. 2010;3(1):92–100.
89. Munch G, Nguyen NT, Nekolla S, et al. Evaluation of sympathetic nerve terminals with [(11)C]epinephrine and [(11)C] hydroxyephedrine and positron emission tomography. Circulation. 2000;101(5):516–23.
90. Schwaiger M, Hutchins GD, Kalff V, et al. Evidence for regional catecholamine uptake and storage sites in the transplanted human heart by positron emission tomography. J Clin Invest. 1991;87 (5):1681–90.
91. Lautamaki R, Tipre D, Bengel FM. Cardiac sympathetic neuronal imaging using PET. Eur J Nucl Med Mol Imaging. 2007;34 Suppl 1:S74–85.
92. Nguyen NT, DeGrado TR, Chakraborty P, Wieland DM, Schwaiger M. Myocardial kinetics of carbon-11-epinephrine in the isolated working rat heart. J Nucl Med. 1997;38(5):780–5.
93. Raffel DM, Corbett JR, del Rosario RB, et al. Sensitivity of [11C] phenylephrine kinetics to monoamine oxidase activity in normal human heart. J Nucl Med. 1999;40(2):232–8.
94. Raffel DM, Corbett JR, del Rosario RB, et al. Clinical evaluation of carbon-11-phenylephrine: MAO-sensitive marker of cardiac sympathetic neurons. J Nucl Med. 1996;37(12):1923–31.
95. Hartmann F, Ziegler S, Nekolla S, et al. Regional patterns of myocardial sympathetic denervation in dilated cardiomyopathy: an analysis using carbon-11 hydroxyephedrine and positron emission tomography. Heart. 1999;81(3):262–70.
96. Vesalainen RK, Pietila M, Tahvanainen KU, et al. Cardiac positron emission tomography imaging with [11C]hydroxyephedrine, a specific tracer for sympathetic nerve endings, and its functional correlates in congestive heart failure. Am J Cardiol. 1999;84 (5):568–74.
97. Pietila M, Malminiemi K, Ukkonen H, et al. Reduced myocardial carbon-11 hydroxyephedrine retention is associated with poor prognosis in chronic heart failure. Eur J Nucl Med. 2001;28(3):373–6.
98. Pietila M, Malminiemi K, Vesalainen R, et al. Exercise training in chronic heart failure: beneficial effects on cardiac (11)C-hydroxyephedrine PET, autonomic nervous control, and ventricular repolarization. J Nucl Med. 2002;43(6):773–9.
99. Bengel FM, Permanetter B, Ungerer M, Nekolla SG, Schwaiger M. Relationship between altered sympathetic innervation, oxidative metabolism and contractile function in the cardiomyopathic human heart; a non-invasive study using positron emission tomography. Eur Heart J. 2001;22(17):1594–600.
100. Pfeffer MA, Braunwald E. Ventricular remodeling after myocardial infarction. Experimental observations and clinical implications. Circulation. 1990;81(4):1161–72.
101. Haubner R, Beer AJ, Wang H, Chen X. Positron emission tomography tracers for imaging angiogenesis. Eur J Nucl Med Mol Imaging. 2010;37 Suppl 1:S86–103.
102. Higuchi T, Bengel FM, Seidl S, et al. Assessment of alphavbeta3 integrin expression after myocardial infarction by positron emission tomography. Cardiovasc Res. 2008;78(2):395–403.
103. Meoli DF, Sadeghi MM, Krassilnikova S, et al. Noninvasive imaging of myocardial angiogenesis following experimental myocardial infarction. J Clin Invest. 2004;113(12):1684–91.
104. Makowski MR, Ebersberger U, Nekolla S, Schwaiger M. In vivo molecular imaging of angiogenesis, targeting alphavbeta3 integrin expression, in a patient after acute myocardial infarction. Eur Heart J. 2008;29(18):2201.
105. Sherif HM, Saraste A, Nekolla SG, et al. Molecular imaging of early alphavbeta3 integrin expression predicts long-term left-ventricle remodeling after myocardial infarction in rats. J Nucl Med. 2012;53(2):318–23.
106. Mann DL, Spinale FG. Activation of matrix metalloproteinases in the failing human heart - Breaking the tie that binds. Circulation. 1998;98(17):1699–702.
107. Nagase H. Activation mechanisms of matrix metalloproteinases. Biol Chem. 1997;378(3–4):151–60.

108. Cottam D, Rees R. Regulation of matrix metalloproteinases - their role in tumor invasion and metastasis. Int J Oncol. 1993;2(6):861–72.
109. Ries C, Petrides PE. Cytokine Regulation of Matrix Metalloproteinase Activity and Its Regulatory Dysfunction in Disease. Biol Chem H-S. 1995;376(6):345–55.
110. Su H, Spinale FG, Dobrucki LW, et al. Noninvasive targeted imaging of matrix metalloproteinase activation in a murine model of postinfarction remodeling. Circulation. 2005;112(20):3157–67.
111. Mukherjee R, Brinsa TA, Dowdy KB, et al. Myocardial infarct expansion and matrix metalloproteinase inhibition. Circulation. 2003;107(4):618–25.
112. Sahul ZH, Mukherjee R, Song J, et al. Targeted imaging of the spatial and temporal variation of matrix metalloproteinase activity in a porcine model of postinfarct remodeling: relationship to myocardial dysfunction. Circ Cardiovasc Imaging. 2011;4(4):381–91.
113. Kang PM, Izumo S. Apoptosis and heart failure: a critical review of the literature. Circ Res. 2000;86(11):1107–13.
114. Terrovitis J, Lautamaki R, Bonios M, et al. Noninvasive quantification and optimization of acute cell retention by in vivo positron emission tomography after intramyocardial cardiac-derived stem cell delivery. J Am Coll Cardiol. 2009;54(17):1619–26.
115. Chan AT, Abraham MR. SPECT and PET to optimize cardiac stem cell therapy. J Nucl Cardiol. 2012;19(1):118–25.
116. Gildehaus FJ, Haasters F, Drosse I, et al. Impact of indium-111 oxine labelling on viability of human mesenchymal stem cells in vitro, and 3D cell-tracking using SPECT/CT in vivo. Mol Imaging Biol. 2011;13(6):1204–14.
117. Higuchi T, Anton M, Dumler K, et al. Combined reporter gene PET and iron oxide MRI for monitoring survival and localization of transplanted cells in the rat heart. J Nucl Med. 2009;50(7):1088–94.
118. Bengel FM. Noninvasive imaging of cardiac gene expression and its future implications for molecular therapy. Mol Imaging Biol. 2005;7(1):22–9.
119. Zhang SJ, Wu JC. Comparison of imaging techniques for tracking cardiac stem cell therapy. J Nucl Med. 2007;48(12):1916–9.
120. Hofmann M, Wollert KC, Meyer GP, et al. Monitoring of bone marrow cell homing into the infarcted human myocardium. Circulation. 2005;111(17):2198–202.